

Article

Accelerated Particle Swarm Optimization for Photovoltaic Maximum Power Point Tracking under Partial Shading Conditions

Muhannad Alshareef ¹, Zhengyu Lin ^{1,*} , Mingyao Ma ² and Wenping Cao ¹ 

¹ Power Electronics, Machine and Power System Group, Aston University, Birmingham B4 7ET, UK; alshareem@aston.ac.uk (M.A.); w.p.cao@aston.ac.uk (W.C.)

² School of Electrical Engineering and Automation, Hefei University of Technology, Hefei 230009, China; miyama@hfut.edu.cn

* Correspondence: z.lin@ieee.org; Tel.: +44-121-204-3722

Received: 23 December 2018; Accepted: 13 February 2019; Published: 15 February 2019



Abstract: This paper presents an accelerated particle swarm optimization (PSO)-based maximum power point tracking (MPPT) algorithm to track global maximum power point (MPP) of photovoltaic (PV) generation under partial shading conditions. Conventional PSO-based MPPT algorithms have common weaknesses of a long convergence time to reach the global MPP and oscillations during the searching. The proposed algorithm includes a standard PSO and a perturb-and-observe algorithm as the accelerator. It has been experimentally tested and compared with conventional MPPT algorithms. Experimental results show that the proposed MPPT method is effective in terms of high reliability, fast dynamic response, and high accuracy in tracking the global MPP.

Keywords: MPPT; partial shading conditions; PV; PSO; P&O

1. Introduction

Rising global energy demands and environmental concerns have led to the fast development of renewable energy technologies. Solar energy as the primary source of renewables can be utilized by Photovoltaics (PV), and has had a rapid growth in the last 30 years [1–5].

PV has a nonlinear electrical characteristic, and it is a challenge to reach PV's optimal performance under changing irradiation conditions. Numerous maximum power point tracking (MPPT) techniques have been developed to maximize the PV output power, such as perturb-and-observe (P&O) and incremental conductance (INC) [6,7]. These conventional MPPT methods are appropriate under uniform irradiation conditions [8,9].

In order to deliver sufficient power, both series and parallel configurations of PV modules are commonly used [10]. In practice, part of the PV arrays can be covered by clouds, leaves, and dust, so partial shading is often unavoidable. Partial shading will greatly reduce the PV module production, and lead to multiple local maximum power points, as shown in Figure 1. The latter effect makes the conventional MPPT algorithms (such as P&O or INC) difficult to track the global MPP [11–13].

In order to find the global MPP under partial shading conditions, many global MPP searching algorithms have been proposed in the literature [14–37].

The MPPT algorithm proposed in [14] is actually an enhancement of the INC algorithm that may find the global MPP by determining all local MPPs. A Fibonacci-based MPPT method is proposed in [15,16], which uses two measured power points to decide the action of the following operating point. Its difference from the P&O methods is that Fibonacci-based MPPT methods change the step size to improve the tracking speed.

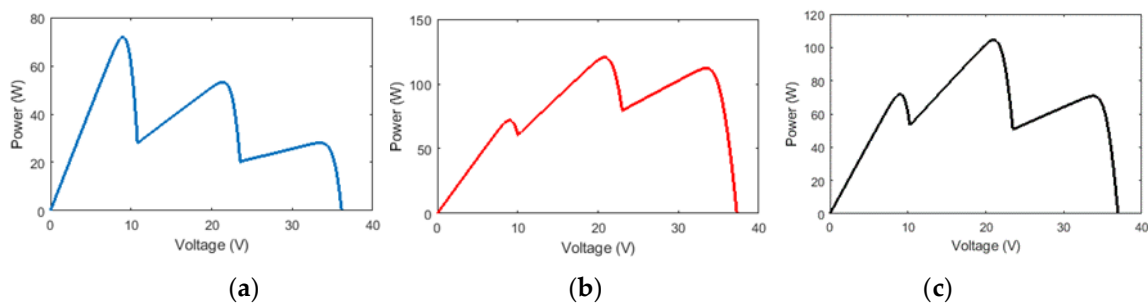


Figure 1. Photovoltaic (PV) output power curves of three different partial shading patterns. (a) partial shading pattern 1; (b) partial shading pattern 2; and (c) partial shading pattern 3.

A partial shading detection method is proposed in [17] by directly measuring each PV module voltage to find mismatch. This strategy is simple and can be easily applied, but it requires a voltage sensor for every PV module, which will increase the system cost. This method is improved in [18] so that the number of local MPPs and their locations can be recognized at the start of scanning process. However, as argued in [19], this method could not find the correct location of local MPPs when a voltage mismatch exists between the modules. In reference [20], it is found that the PV current can be influenced by partial shading conditions. However, this particular relationship is not always accurate, as argued in [21]. The MPPT method proposed in [22] is simply a P&O algorithm, and its voltage step sizes is solely based on dividing rectangles technique. However, this method does not ensure attainment of the global MPP. A neural-network-based MPPT for various partial shading conditions is presented in [23]. The main drawback of this system is that it requires the measurement of the sun irradiance and PV module's temperature.

In reference [24], a two-stage MPPT technique is proposed. The first stage is to move the operating point near the MPP before it converges to the MPP in the second stage. This method added more complexity to the system, which needs more circuits for open circuit voltage and short circuit current measurements. In addition, this method does not guarantee to track the global MPP under partial shading conditions. In reference [25], it is proposed that every PV module is connected to a DC–DC converter (PV power optimizer) so that each PV module will work on the MPP, and the total PV array output power could be optimized. The main drawback of this arrangement is the high cost of the PV system.

Artificial intelligence (AI)-based MPPT algorithms are proposed in [26–29], which include particle swarm optimization (PSO), ant colony, and firefly algorithms. The PSO algorithm is popular for MPPT because of its simplicity of the mathematical structure and implementation [30,31].

Several PSO-based MPPT algorithms [32,33] have been developed for PV systems to resolve the multiple local MPP problems. However, as claimed in [34], one particular issue of the PSO based MPPT algorithm is the long tracking time toward the MPP within large search spaces. A hybrid PSO-based MPPT was proposed to identify the global MPP in several nearby peaks [35]. A simplified PSO-based MPPT algorithm is proposed in [36] to simplify the search approach. However, in the abovementioned PSO-based MPPT algorithms, the global MPP searching restarting issue is not discussed, which is required when the shading patterns change.

This paper proposes an accelerated PSO (APSO) based MPPT algorithm. The particle with the highest fitness value (PV power) is perturbed by a P&O MPPT algorithm to search for the global MPP so that the best particle moves faster to the global MPP, and at the same time attracts the remaining particles to converge toward it more quickly. Hence, the search time needed for convergence could be significantly reduced. Additionally, there is no need to add any constraint on the optimal particle velocity. The proposed strategy can improve MPPT effectiveness without adding any additional complexity.

The rest of this paper is organized as follows. The standard PSO strategy is briefly introduced in Section 2. Section 3 subsequently describes the proposed APSO approach. Experimental results of

using the proposed algorithm and other MPPT algorithms are presented and compared in Section 4. Finally, conclusions are given in Section 5.

2. Overview of Particle Swarm Optimization Algorithm

In 1995, Eberhart and Kennedy first proposed particle swarm optimization (PSO) algorithm, which was motivated by bird flocking and fish schooling [33] to deal with issues where the best solution can be represented in point or on a surface in a dimensional space. Numerous particles (agents) are employed in PSO algorithm, and each agent can share the information within their own search process. There are two basic rules need to be followed by each particle: tracking the most effective performing particle, and determining the optimum conditions acquired by the particle itself.

By following the above two rules, each particle can eventually progress to the optimal solution. The following two equations can be used to characterize the standard PSO method:

$$\theta_i^{k+1} = w\theta_i^k + c_1r_1 [P_{best} - X_i^k] + c_2r_2 [G_{best} - X_i^k] \quad (1)$$

$$X_i^{k+1} = X_i^k + \theta_i^{k+1} \quad (2)$$

where X_i^k is the position of the particle i , and θ_i^k represents its velocity. The iteration number is denoted by k , and w is the inertia weight. r_1 and r_2 are random values distributed within $[0, 1]$, and the cognitive and social coefficients are described by c_1 and c_2 , respectively. P_{best} is used to store the best experience by the particle itself, and the best position of all particles is kept in G_{best} .

For a DC to DC power converter, assuming the output voltage is a constant, the input voltage (i.e., PV voltage) can be calculated from the output voltage V_o and the duty cycle d . For example, for a Boost converter used in this research, the input voltage can be calculated as:

$$V_{in} = V_o \times (1 - d) \quad (3)$$

Therefore, to apply PSO algorithm in PV applications, the particle position (X_i^k) in Equations (1) and (2) can be considered as the duty cycle (d_i^k) of the PV converter, while the velocity (θ_i^k) can be considered as the change of the duty cycle (Δd_i^k). Therefore, PSO method for MPPT can be expressed by Equations (4) and (5):

$$\Delta d_i^{k+1} = w\Delta d_i^k + c_1r_1 [P_{best} - d_i^k] + c_2r_2 [G_{best} - d_i^k] \quad (4)$$

$$d_i^{k+1} = d_i^k + \Delta d_i^{k+1} \quad (5)$$

The change of the duty cycle Δd_i^k is influenced by two variables: the best solution founded by the particle itself (P_{best}), and the best solution in the entire population (G_{best}). If the current duty cycle d_i^k is far away from these two values, it will be updated by a large velocity. When the condition in Equation (7) is satisfied, P_{best} in Equation (6) will be updated; otherwise, P_{best} retains its present value. Then, the fitness value of each particle will be evaluated to see if G_{best} value needs to be updated.

$$P_{best} = d_i^k \quad (6)$$

$$f(d_i^k) > f(P_{best}) \quad (7)$$

where f is the objective function that should be maximized.

The flowchart of the standard PSO algorithm is shown in Figure 2, and each step is described as follows:

Step 1: Initialize the particles randomly in the search space.

Step 2: Evaluate the fitness value of each particle by sending the candidate solution to the objective function.

Step 3: Update P_{best} and G_{best} .

Step 4: Update the position and velocity of each particle.

Step 5: Re-initialize the PSO algorithm unless the constrain is met. In other words, the algorithm stops when the G_{best} is founded.

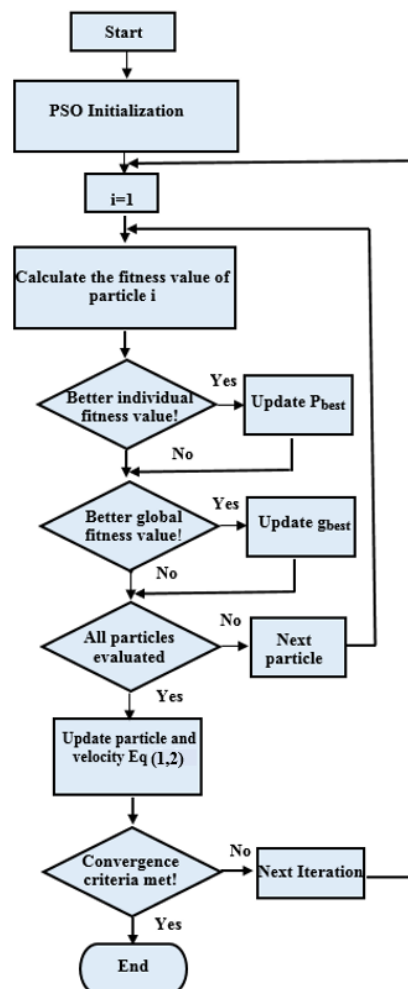


Figure 2. Flowchart of the standard particle swarm optimization (PSO) method.

Figure 3 shows how a standard PSO algorithm scan the P–V curve of a PV module to find the global maximum power point under partial shading conditions. The P–V curve in Figure 3 has three local MPPs. Firstly, three initial duty cycles (particles) are given as follow: $X_1 = 0.2$, $X_2 = 0.5$, $X_3 = 0.8$. The output PV power is selected as the fitness function value to be maximized.

The PSO algorithm operates the PV Boost converter under these three duty cycles (position of particles), and the PV voltage and PV current can be measured for each duty cycle. Then, the PV output power (fitness value) can be calculated. The particle X_2 is served as G_{best} because it has the highest PV output power (as shown in Figure 3a). The velocity Δd_i^{k+1} and position d_i^{k+1} of each particle is updated accordingly after the first iteration.

After updating three duty cycle values, new PV output power for each duty cycle can be obtained in the second iteration. As shown in Figure 3b, it can be seen that X_2 is still the best particle. It is worth noting that as soon as the particles move to G_{best} , the velocity becomes smaller. Since all duty cycles achieve higher PV output power, the velocity direction of these particles remains unchanged and moved to G_{best} . After several interactions, it can be observed that all particles reach global MPP (GMPP) after several iterations, as shown in Figure 3c.

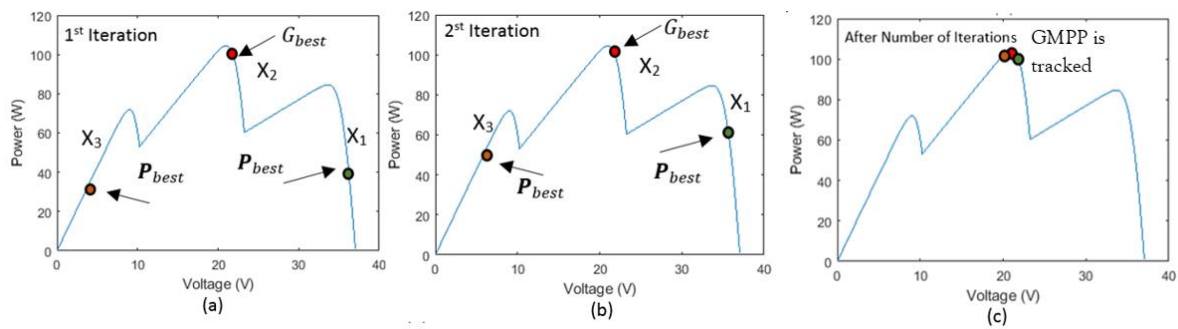


Figure 3. How a standard PSO algorithm scan the P–V curve of a photovoltaic (PV) module to find global maximum power point (GMPP).

3. Proposed Accelerated PSO Algorithm

As discussed in Section 2, the PV power converter pulse width modulation (PWM) duty cycle d is selected to represent the particle position in the proposed APSO algorithm, and the output power of the PV array is selected as the fitness function value.

The flowchart of the proposed APSO algorithm is shown in Figure 4, and the main steps are discussed in detail as follow:

- Step 1 (Parameter Selection): The number of particles is three. A complete optimization analysis has been done in [24], and it claimed that three particles deliver the best performance.
- Step 2 (APSO Initialization): In the proposed APSO algorithm, the particles are placed on fixed positions. The first particle is set as 10% of the PV open circuit voltage (V_{oc}), the third particle is set as 90% of V_{oc} . The first and third particles defined the PSO search space. The second particle is randomly set between 10% and 90% of V_{oc} .
- Step 3 (Fitness Evaluation): The purpose of the PSO-based MPPT method is to maximize the PV output power. PV voltage and current are measured to compute the PV output power as the fitness value for evaluation.
- Step 4 (Update the Global Value): The particle which has the best fitness value is selected as the G_{best} . In conventional PSO-based MPPT algorithms, G_{best} is usually fixed. In this proposed APSO method, P&O MPPT algorithm is used to directly perturb the G_{best} to accelerate the global MPP searching, so that G_{best} will be moved towards a higher fitness value. In conventional PSO-based MPPT algorithms, the velocity of the particle is reducing when the particle is moving toward the G_{best} . In this proposed APSO method, G_{best} can move to a higher fitness value via P&O algorithm, and simultaneously attracts the remaining particle more rapidly to converge toward it. Therefore, the convergence time could be decreased.

Also, in this proposed APSO method, there is no need to search for local best P_{best} . So, Equation (4) can be modified to (8), and the convergence of the algorithm only depends on the G_{best} . Furthermore, the new equation will reduce the calculation complexity.

$$\Delta d_i^{k+1} = w\Delta d_i^k + \beta [G_{best} - d_i^k] \quad (8)$$

where $\beta = 0.1\text{--}0.7$, which is the coefficient.

So, the new particle position can be determined as Equation (9):

$$d_i^{k+1} = w\Delta d_i^k + (1 - \beta)d_i^k + \beta G_{best} \quad (9)$$

- Step 5 (Update the Velocity and Position of Each Particle): Once all the particles are assessed, the position and velocity of each particle need to be updated.

- Step 6 (Convergence Determination): Two convergence criteria will be examined in this step. If the particle's velocity becomes lower than a set value or if the maximum iteration number is reached, the algorithm computation will be stopped, and the global MPP is found.
- Step 7 (Re-initialization): The global MPP position frequently changes with the environmental conditions. This requires the APSO algorithm to be reinitialized and search for the new global MPP. In this research, Equation (10) is used to identify the environmental conditions changes and reinitialize the APSO algorithm.

$$\frac{P_{PV, new} - P_{PV, last}}{P_{PV, last}} > \Delta P(\%) \quad (10)$$

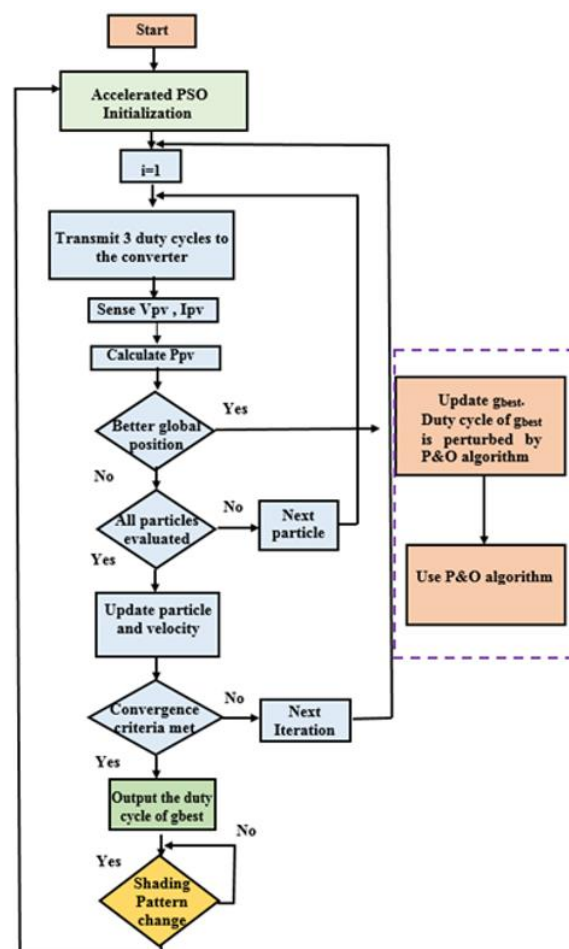


Figure 4. Flowchart of the proposed accelerated PSO (APSO) algorithm.

The operating principle of the proposed APSO algorithm is demonstrated in Figure 5. Three PWM duty cycles (particles) of the PV power converter were selected, as shown in Figure 5a. The first and third particles defined the MPP searching range of APSO method. Then, the fitness function value (PV output power) of all the three particles is evaluated. Then, one optimal duty cycle (G_{best}) is identified, say at $X_2 = 0.60$. During the first iteration, particles X_1 and X_3 followed the optimal particle position X_2 to arrive at their new location for the next iteration. X_2 represents the particle with the highest fitness value (G_{best}). P&O algorithm is employed to move X_2 toward the global MPP. By end of this iteration, X_2 value is also updated, as shown in Figure 5b. The particles position and velocity of the three particles are updated via more iterations.

It is observed that the proposed method identifies the GMPP at the end of the second iteration ($X_2 = 0.52$) as shown in Figure 5c. This process continues until particles X_1 and X_3 reach the global MPP as

illustrated in Figure 5d. The proposed APSO algorithm can move the operating point to the global MPP quicker and has faster convergence speed compared to the conventional PSO algorithm. If a large change of environmental condition is detected, the particles (duty cycles) will be re-initialized, and the APSO algorithm is run again to search for the new global MPP.

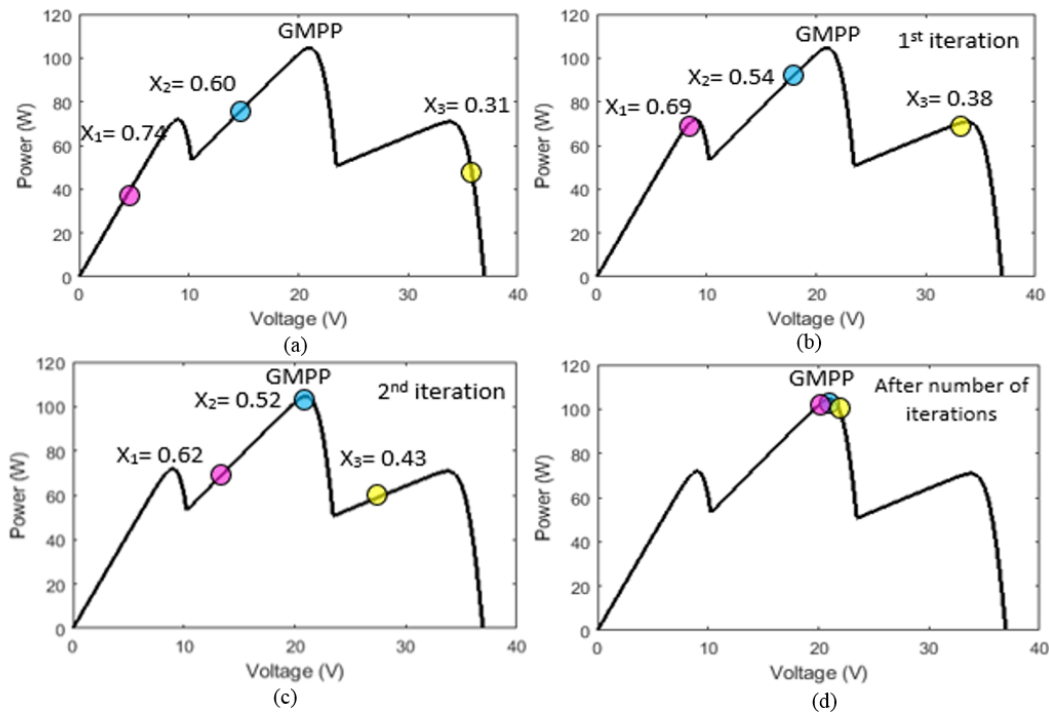


Figure 5. (a) Particles are initialized on a PV curve. (b) New position of particles after first iteration. (c) Particle X_2 reaches GMPP by the end of second iteration. (d) All particles are approaching the GMPP.

4. Experimental Results

4.1. Experimental Setup Configuration

The performance of the proposed APSO method is verified experimentally. The experimental setup is shown in Figures 6 and 7, which includes a PV simulator (Chroma 62050H-600S Programmable DC Power Supply) as the PV source, four 12 V VRLA batteries as the energy storage, and a 200 W Boost converter as the PV power converter. The proposed APSO method was implemented in a TMS320F28335 microcontroller. The PV simulator can mimic the behavior of PV array exposed to various shading patterns, as shown in Figure 1.

4.2. Setting the Parameter Values of the Particle Swarm Optimization Algorithm

The parameters of MPPT methods in comparison study are shown in Table 1. They are determined through offline simulation. The search starting point for P&O algorithm is set as the duty cycle of 0.2.

Table 1. Parameters of MPPT methods in comparison study.

Parameter	P&O	PSO	Proposed APSO
Number of Particles	$d = 0.2$	3	3
w	$\Delta d = 0.01$	0.4	—
c_1	—	1.2	—
c_2	—	1.4	—
β	—	—	0.1–0.7
Sampling time	0.12 s	0.12 s	0.12 s

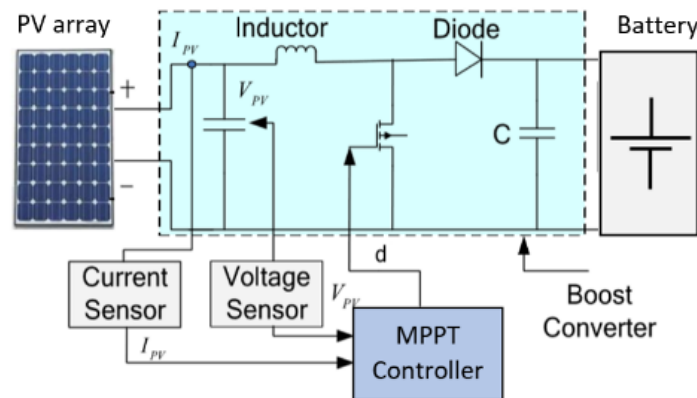


Figure 6. Block diagram of the PV system experimental setup.

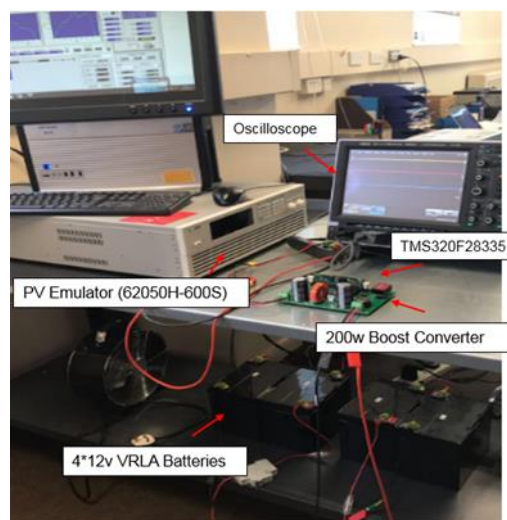


Figure 7. Photograph of the experimental setup.

4.3. Case Studies

To evaluate the proposed APSO algorithm and compare it with different MPPT algorithms under various shading patterns, three test scenarios have been defined in this study. In the experiments, the voltage and current are measured through the oscilloscope readings. The voltage measurement V_m has a typical uncertainty ΔV_m of ± 0.3 V, and the current measurement I_m has a typical uncertainty ΔI_m of ± 10 mA. The power measurement uncertainty ΔP_m can be obtained by:

$$\Delta P_m \cong V_m \Delta I_m + I_m \Delta V_m \quad (11)$$

In this research, the typical power measurement uncertainty is between ± 0.5 to ± 1.0 W.

Scenario 1: PV output has three MPPs, and the GMPP occurs in the middle at $V = 23$ V, as shown in Figure 8. The experiment results of the voltage, current, and power waveforms for this scenario are shown in Figure 9. It was noticed that the proposed APSO algorithm reached the GMPP in 2.4 s with PV output power 40.56 W (Figure 9a). The conventional PSO algorithm took longer time with 4.6 s and GMPP is about 39.44 W (Figure 9b). On the other hand, it takes 3.2 s to reach GMPP using Simplified PSO method in [36] with PV output power 40.37 W (Figure 9c). However, the P&O algorithm got trapped at the right local MPP with 35.87 W (Figure 9d). Also, the oscillation can be observable in this method. From the experiment results, it is clearly that the proposed APSO method has a quicker convergence speed than the standard PSO algorithm.

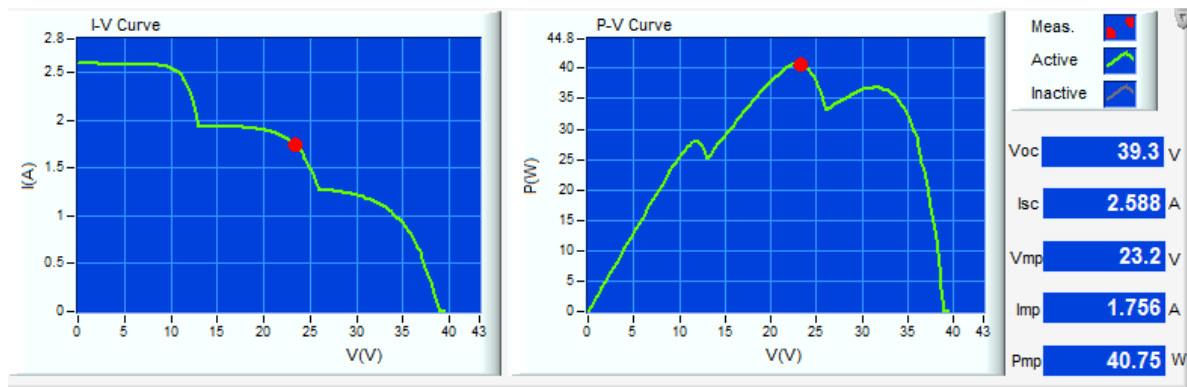


Figure 8. P-V and I-V curves of Scenario 1.

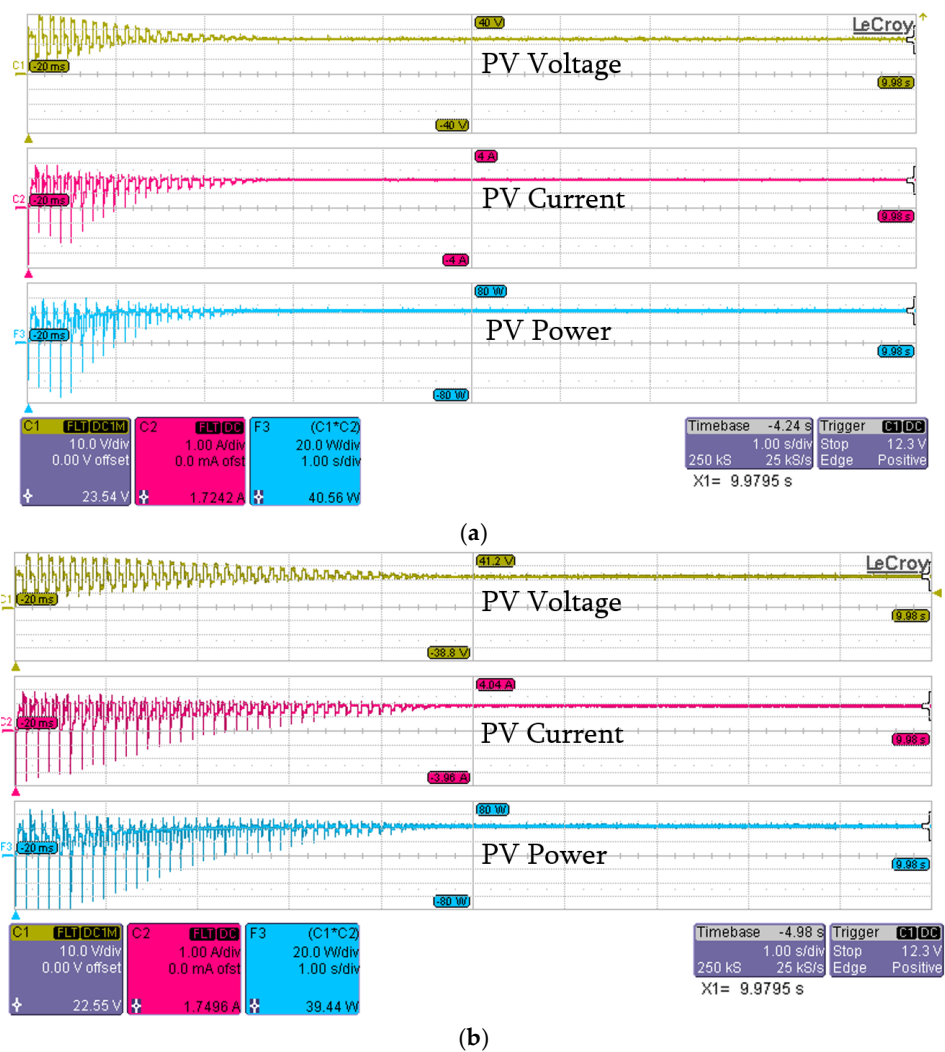


Figure 9. Cont.

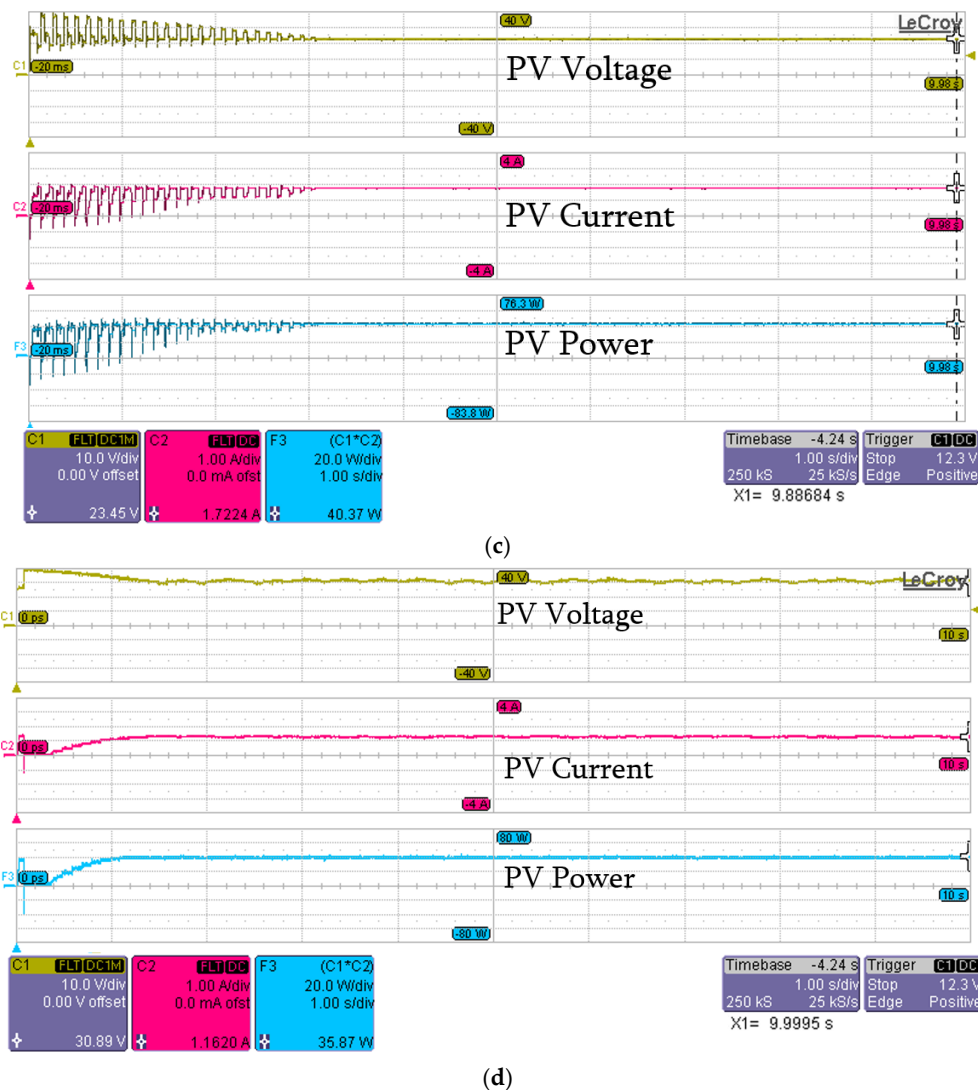


Figure 9. Convergence characteristics of (a) Proposed APSO, (b) PSO, (c) Simplified PSO in [36], and (d) P&O under Scenario 1.

Scenario 2: In this scenario, PV output has three MPPs, and the GMPP occurs in the highest voltage at $V = 32\text{V}$ (As shown in Figure 10). The experiment results for four MPPT algorithms as described in scenario 2 can be found in Figure 11. It was noticed that the proposed APSO algorithm rapidly identifies the GMPP in just 1.9 s, and output power is 73.33 W. Standard PSO algorithm was able to climb to the GMPP within 3 s for the same PV output power. On the other hand, it takes 2.8 s to track GMPP using Simplified PSO method in [36] with PV output power 70.31 W. In this scenario, the P&O algorithm can track the GMPP when its initial duty cycle value is set as 0.2, and the output power is 72.00 W.

It should be noted that whether the P&O algorithm can track the GMPP depends on the search starting point. For example, if the search starting point is from the duty cycle of 0.6 in this scenario, the P&O algorithm will not find the GMPP.

Scenario 3: In this scenario, the PV has two MPPs (Figure 12). Four different algorithms were tested, and the experimental results are shown in Figure 13. The output PV power of the proposed APSO algorithm is about 76.51 W and reaches GMPP within 2.3 s. On the other hand, the standard PSO method arrived to the GMPP with convergence time 4.2 s and with 72.17 W. It takes 3.2 s to acquire the GMPP with Simplified PSO method [36] and PV output power is about 76.39 W. The P&O method got caught in one of the local MPPs and PV output power is about 44.1 W.

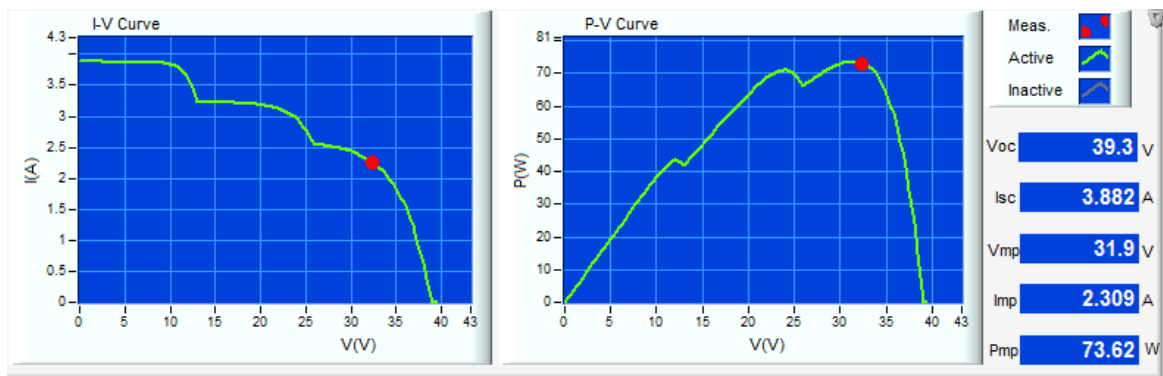


Figure 10. P-V and I-V curves for Scenario 2.

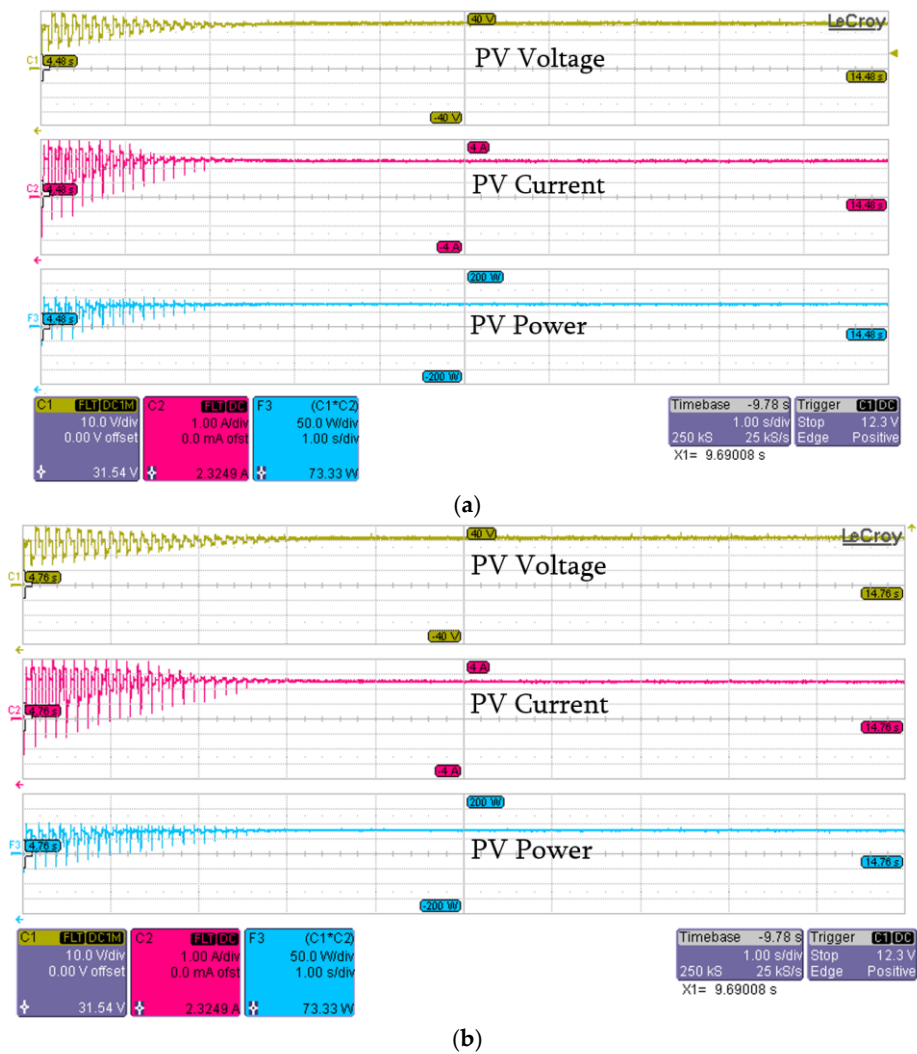
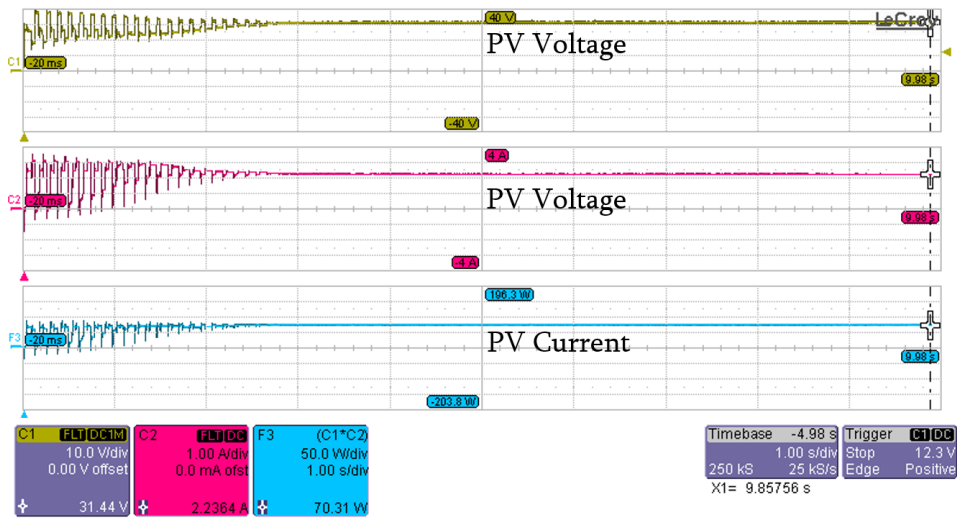
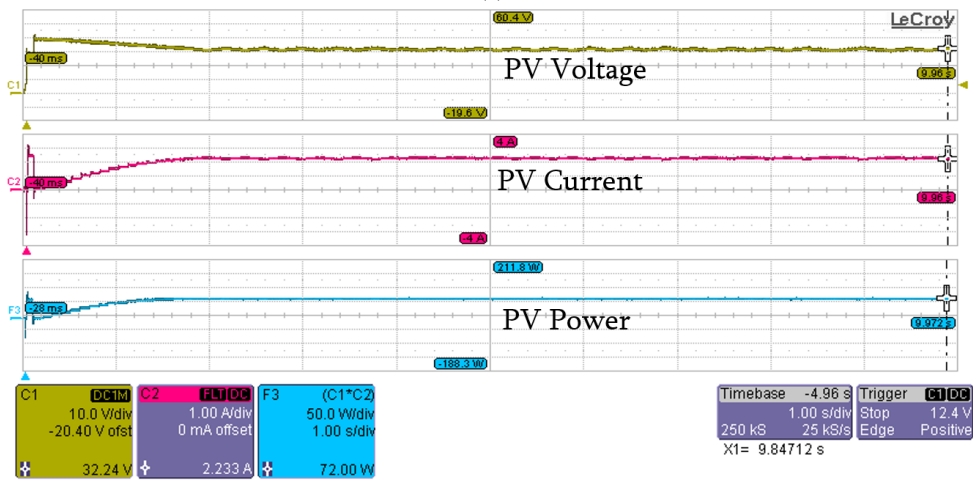


Figure 11. Cont.



(c)



(d)

Figure 11. Convergence characteristics of (a) Proposed APSO, (b) PSO, (c) Simplified PSO in [36], and (d) P&O under Scenario 2.

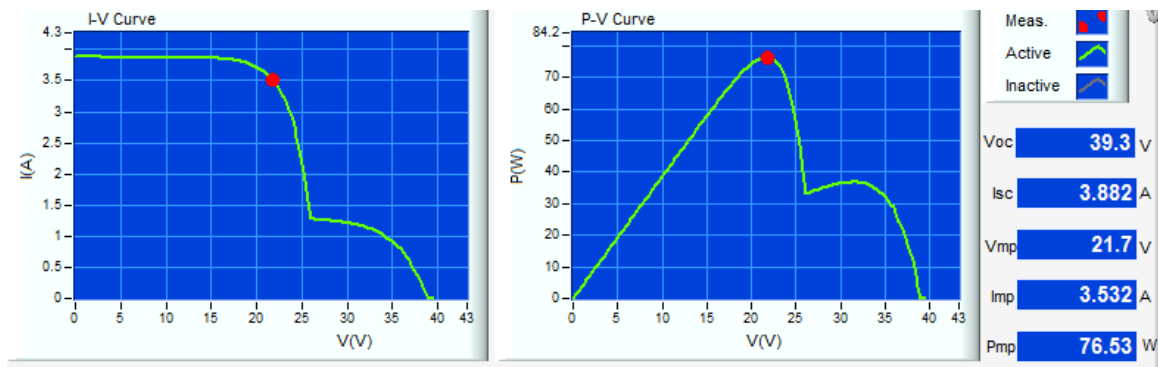
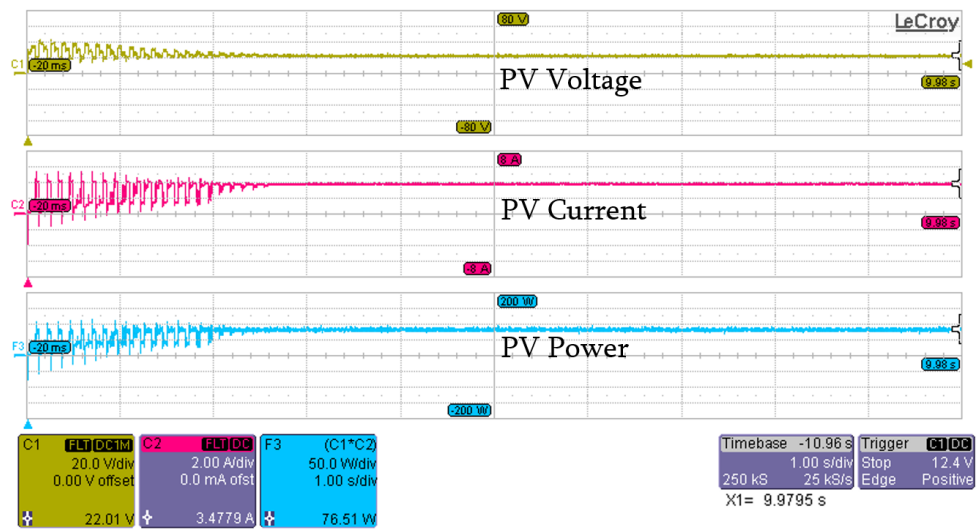
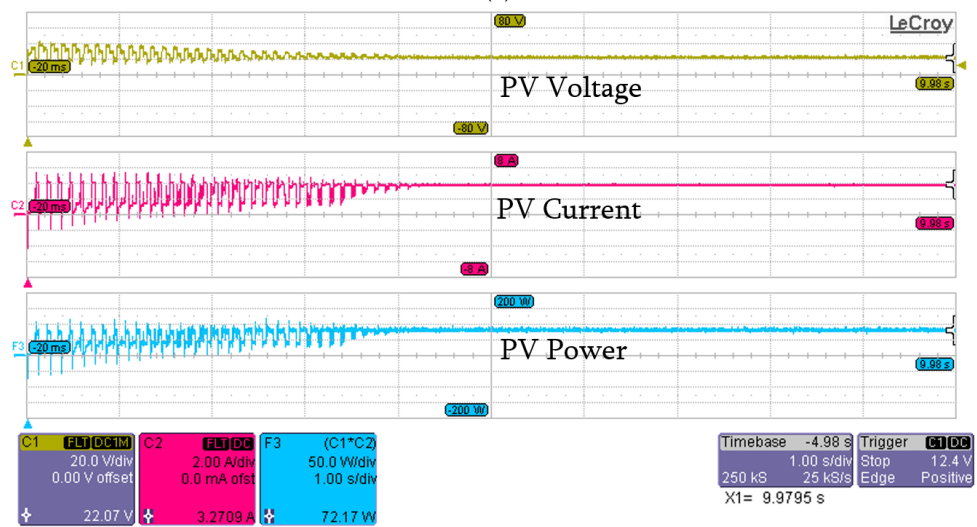


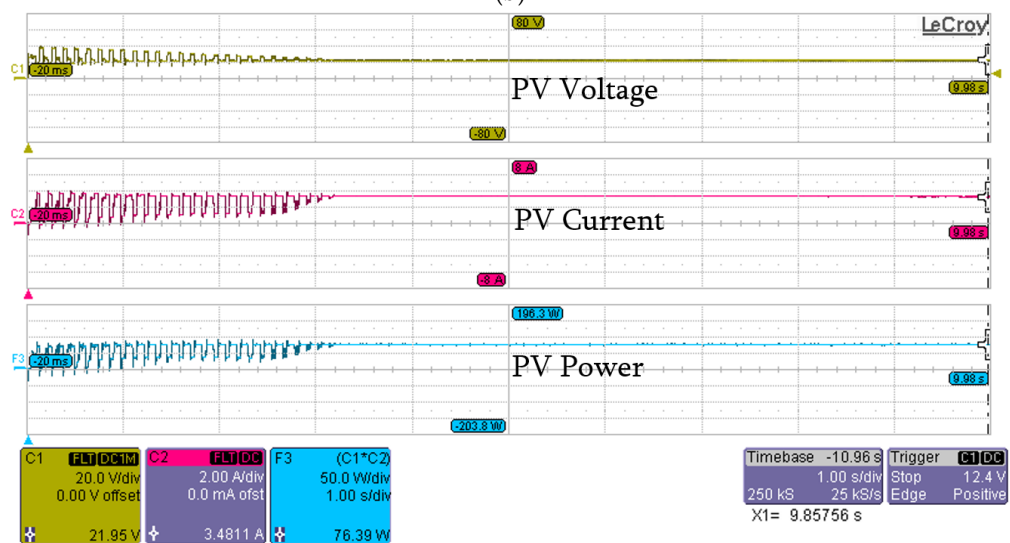
Figure 12. P-V and I-V curves of Scenario 3.



(a)

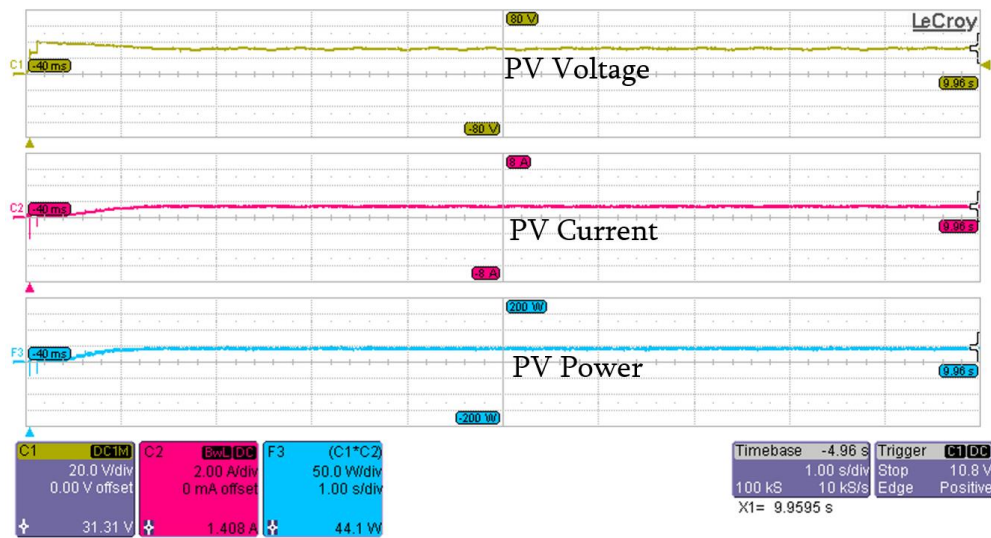


(b)



(c)

Figure 13. Cont.



(d)

Figure 13. Convergence characteristics of (a) Proposed APSO, (b) PSO, (c) Simplified PSO in [36], and (d) P&O under Scenario 3.

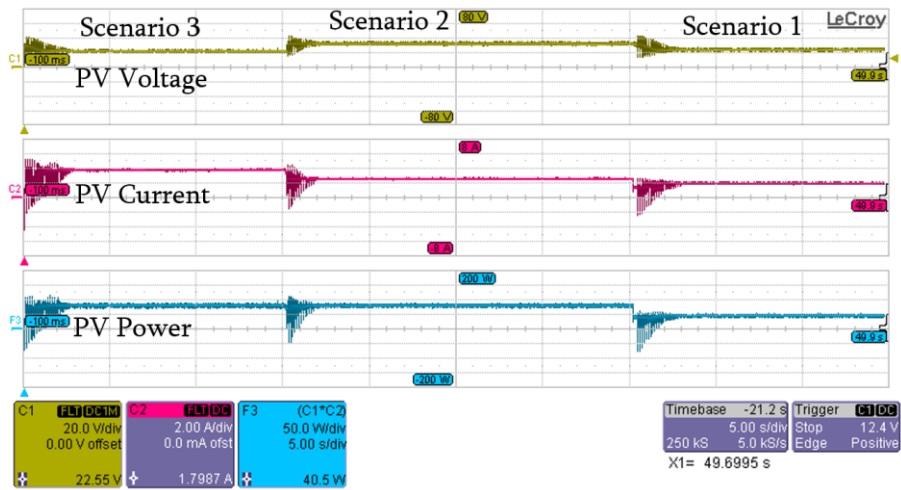
Table 2 summarized the comparison experimental results of four MPPT algorithm.

Table 2. Summary of Comparison results of APSO, PSO, simplified PSO in [36], and P&O methods in terms of power tracked, efficiency, and tracking time.

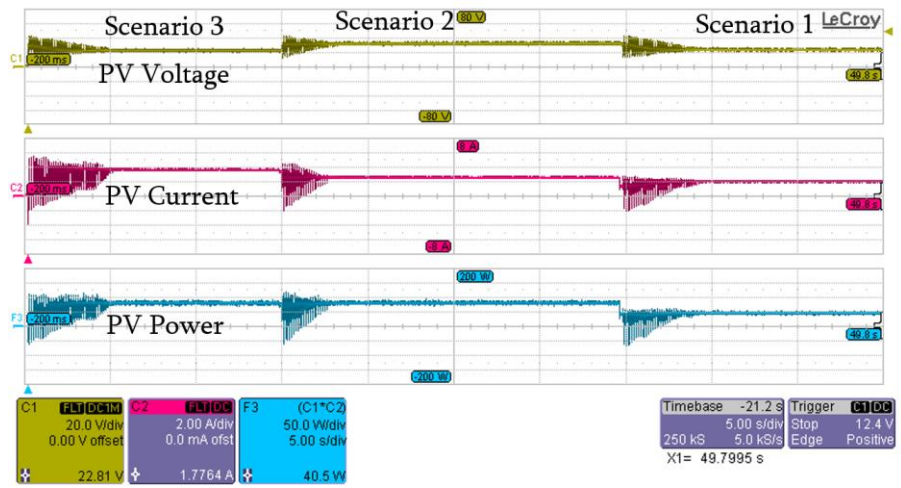
Shading Scenario	Method	V_{mpp} (V)	I_{mpp} (A)	P_{mpp} (W)	Rated Power (W)	Efficiency (%)	Tracking Time (s)
Scenario (1)	APSO	23.54	1.72	40.56	40.76	99	2.4
	PSO	22.55	1.75	39.44		97	4.6
	PSO [36]	23.45	1.72	40.37		99	3.2
	P&O	30.89	1.16	35.87		76	1.1
Scenario (2)	APSO	31.54	2.32	73.33	73.62	99	1.9
	PSO	31.54	2.3	73.33		99	3
	PSO [36]	31.44	2.23	70.31		96	2.8
	P&O	32.24	2.233	72.00		98	1.9
Scenario (3)	APSO	22.01	3.47	76.51	76.53	99	2.3
	PSO	22.07	3.27	72.17		94	4.2
	PSO [36]	21.95	3.48	76.39		99	3.2
	P&O	31.31	1.41	44.1		58	1.2

4.4. Test under Partial Shading Variations

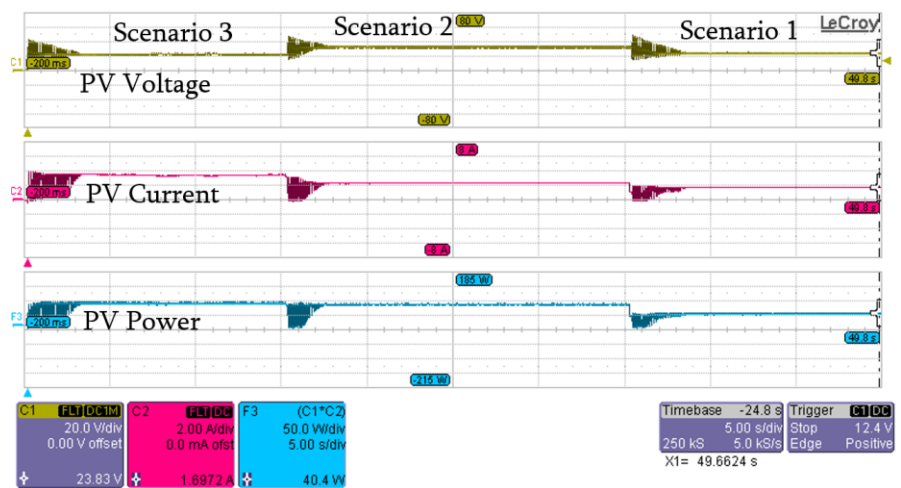
The proposed APSO was also tested under the variation of partial shading patterns. In this experiment, the shaded pattern is changed from scenario 3 to scenario 2 and then to scenario 1. Figure 14a–d show the experiment results of the proposed APSO, PSO, Simplified PSO in [36], and P&O MPPT, respectively. After detecting the occurrence of partial shading, P&O reaches the GMPP rapidly (scenario 2). However, it got trapped in one of the local MPPs once the shaded pattern was changed from scenario 2 to scenario 1. The experiment results show that the proposed APSO algorithm is very sensitive to any variation in shaded patterns. On the other hand, the standard PSO algorithm suffers from large oscillation before it reaches the MPP. Moreover, its convergence time is longer than the proposed APSO algorithm. The experiment results indicate that the proposed APSO can track GMPP successfully within a shorter time and exhibit lower oscillations during the transients than the standard PSO algorithm.



(a)

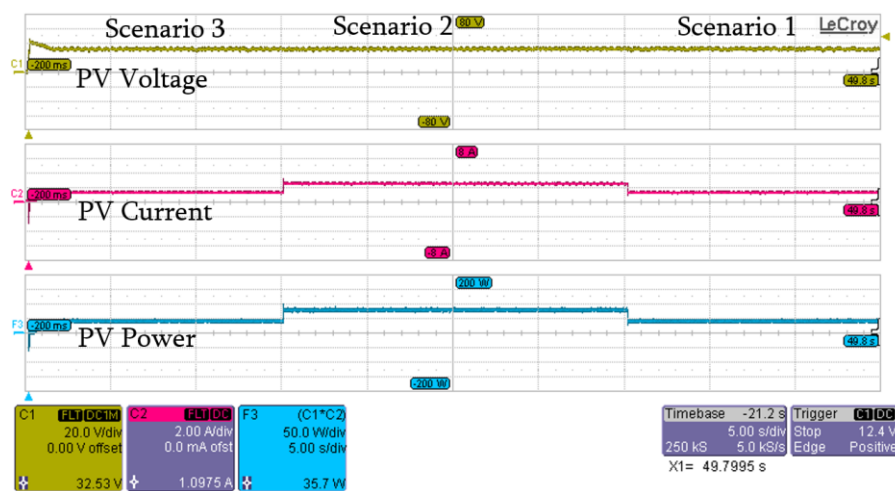


(b)



(c)

Figure 14. Cont.



(d)

Figure 14. Convergence Characteristics of (a) Proposed PSO, (b) PSO, (c) Simplified PSO in [36], and (d) P&O under changing partial shading conditions.

5. Conclusions

This paper presents an accelerated particle-swarm-optimization-based MPPT technique to track the global MPP for a PV system under partial shading conditions. The proposed algorithm has a combination of PSO and P&O MPPT algorithms to accelerate the MPP searching, and it is verified through experiments under various partial shading conditions. According to the experiment results, the proposed APSO algorithm can clearly distinguish the GMPP from local MPPs in all test scenarios, including the change of shading patterns. Compared to the conventional PSO algorithm, the proposed algorithm offers higher convergence speed and better dynamic response.

Author Contributions: Conceptualization, M.A. and Z.L.; methodology, M.A., Z.L. and W.C.; simulation and experimental validation, M.A., Z.L., M.M. and W.C.; writing—original draft preparation, M.A.; writing—review and editing, Z.L., M.M., and W.C.; supervision, Z.L.; funding acquisition, M.A., Z.L. and M.M.

Funding: This research has received scholarship from Saudi Arabia Cultural Bureau in the UK and funding from the European Union’s Horizon 2020 research and innovation programme under grant agreement No. 734796.

Conflicts of Interest: The authors declare no conflict of interest.

References

1. Chiu, H.J.; Lo, Y.K.; Yao, C.J.; Lee, T.P.; Wang, J.M.; Lee, J.X. A Modular Self-Controlled Photovoltaic Charger with Inter Integrated Circuit (I2C) Interface. *IEEE Trans. Energy Convers.* **2011**, *26*, 281–289. [\[CrossRef\]](#)
2. Farivar, G.; Asaei, B. A New Approach for Solar Module Temperature Estimation Using the Simple Diode Model. *IEEE Trans. Energy Convers.* **2011**, *26*, 1118–1126. [\[CrossRef\]](#)
3. Lopez-Lapena, O.; Penella, M.; Gasulla, M. A Closed-Loop Maximum Power Point Tracker for Subwatt Photovoltaic Panels. *IEEE Trans. Ind. Electron.* **2012**, *59*, 1588–1596. [\[CrossRef\]](#)
4. Mäki, A.; Valkealahti, S. Power Losses in Long String and Parallel-Connected Short Strings of Series-Connected Silicon-Based Photovoltaic Modules Due to Partial Shading Conditions. *IEEE Trans. Energy Convers.* **2012**, *27*, 173–183. [\[CrossRef\]](#)
5. Thounthong, P. Model Based-Energy Control of a Solar Power Plant with a Supercapacitor for Grid-Independent Applications. *IEEE Trans. Energy Convers.* **2011**, *26*, 1210–1218. [\[CrossRef\]](#)
6. Bidram, A.; Davoudi, A.; Balog, R. Control and Circuit Techniques to Mitigate Partial Shading Effects in Photovoltaic Arrays. *IEEE J. Photovolt.* **2012**, *2*, 532–546. [\[CrossRef\]](#)
7. Soon, K.; Mekhilef, S.; Safari, A. Simple and low cost incremental conductance maximum power point tracking using buck-boost converter. *J. Renew. Sustain. Energy* **2013**, *5*, 023106.

8. Kjær, S.B. Evaluation of the Hill Climbing and the Incremental Conductance Maximum Power Point Trackers for Photovoltaic Power Systems. *IEEE Trans. Energy Convers.* **2012**, *27*, 922–929. [[CrossRef](#)]
9. Sera, D.; Mathe, L.; Kerekes, T.; Spataru, S.; Teodorescu, R. On the Perturb-and-Observe and Incremental Conductance MPPT Methods for PV Systems. *IEEE J. Photovolt.* **2013**, *3*, 1070–1078. [[CrossRef](#)]
10. Salas, V.; Olias, E.; Barrado, A.; Lazaro, A. Review of the maximum power point tracking algorithms for stand-alone photovoltaic systems. *Sol. Energy Mater. Sol. Cells* **2006**, *90*, 1555–1578. [[CrossRef](#)]
11. Kollimalla, S.K.; Mishra, M.K. Variable perturbation size adaptive P&O MPPT algorithm for sudden changes in irradiance. *IEEE Trans. Sustain. Energy* **2014**, *5*, 718–728.
12. Kok Soon, T.; Mekhilef, S. Modified incremental conductance algorithm for photovoltaic system under partial shading conditions and load variation. *IEEE Trans. Ind. Electron.* **2014**, *61*, 5384–5392. [[CrossRef](#)]
13. Lyden, S.; Haque, M.E. Comparison of the perturb and observe and simulated annealing approaches for maximum power point tracking in a photovoltaic system under partial shading conditions. In Proceedings of the 2014 IEEE Energy Conversion Congress and Exposition (ECCE), Pittsburgh, PA, USA, 14–18 September 2014; pp. 2517–2523.
14. Ji, Y.H.; Jung, D.Y.; Kim, J.G.; Kim, J.H.; Lee, T.W.; Won, C.Y. A real maximum power point tracking method for mismatching compensation in PV array under partially shaded conditions. *IEEE Trans. Power Electron.* **2011**, *26*, 1001–1009. [[CrossRef](#)]
15. Ahmed, N.A.; Miyatake, M. A novel maximum power point tracking for photovoltaic applications under partially shaded insolation conditions. *Electr. Power Syst. Res.* **2008**, *78*, 777–784. [[CrossRef](#)]
16. Miyatake, M.; Inada, M.T.; Hiratsuka, I.; Zhao, H.; Otsuka, H.; Nakano, M. Control characteristics of a fibonacci-search-based maximum power point tracker when a photovoltaic array is partially shaded. In Proceedings of the 4th International Power Electronics Motion Control Conference (IPEMC'04), Xi'an, China, 14–16 August 2004; pp. 816–821.
17. Kai, C.; Shulin, T.; Yuhua, C.; Libing, B. An improved MPPT controller for photovoltaic system under partial shading condition. *IEEE Trans. Sustain. Energy* **2014**, *5*, 978–985.
18. Patel, H.; Agarwal, V. Maximum Power Point Tracking Scheme for PV Systems Operating Under Partially Shaded Conditions. *IEEE Trans. Ind. Electron.* **2008**, *55*, 1689–1698. [[CrossRef](#)]
19. Spertino, F.; Ahmad, J.; Di Leo, P.; Ciocia, A. A method for obtaining the I-V curve of photovoltaic arrays from module voltages and its applications for MPP tracking. *Sol. Energy* **2016**, *139*, 489–505. [[CrossRef](#)]
20. Kouchaki, A.; Iman-Eini, H.; Asaei, B. A new maximum power point tracking strategy for PV arrays under uniform and non-uniform insolation conditions. *Sol. Energy* **2013**, *91*, 221–232. [[CrossRef](#)]
21. Ahmed, J.; Salam, Z. An improved method to predict the position of maximum power point during partial shading for PV arrays. *IEEE Trans. Ind. Inform.* **2015**, *11*, 1378–1387. [[CrossRef](#)]
22. Tat Luat, N.; Kay-Soon, L. A global maximum power point tracking scheme employing direct search algorithm for photovoltaic systems. *IEEE Trans. Ind. Electron.* **2010**, *57*, 3456–3467.
23. Syafaruddin, S.; Karatepe, E.; Hiyama, T. Artificial neural network polar coordinated fuzzy controller based maximum power point tracking control under partially shaded conditions. *IET Renew. Power Gener.* **2009**, *3*, 239–253. [[CrossRef](#)]
24. Kobayashi, K.; Takano, I.; Sawada, Y. A study on a two-stage maximum power point tracking control of a photovoltaic system under partially shaded isolation conditions. In Proceedings of the IEEE Power Engineering Society General Meeting Conference, Toronto, ON, Canada, 13–17 July 2003; pp. 2612–2617.
25. Femia, N.; Gianpaolo, L.; Giovanni, P.; Spagnuolo, G.; Vitelli, M. Distributed maximum power point tracking of photovoltaic arrays: Novel approach and system analysis. *IEEE Trans. Ind. Electron.* **2008**, *55*, 2610–2621. [[CrossRef](#)]
26. Yetayew, T.T.; Jyothsna, T.R.; Kusuma, G. Evaluation of Incremental conductance and Firefly algorithm for PV MPPT application under partial shade condition. In Proceedings of the IEEE 6th International Conference on Power Systems (ICPS), New Delhi, India, 4–6 March 2016; pp. 1–6.
27. Teshome, D.F.; Lee, C.H.; Lin, Y.W.; Lian, K.L. A Modified Firefly Algorithm for Photovoltaic Maximum Power Point Tracking Control under Partial Shading. *IEEE J. Emerg. Sel. Top. Power Electron.* **2017**, *5*, 661–671. [[CrossRef](#)]

28. Phimmason, V.; Endo, T.; Kondo, Y.; Miyatake, M. Improvement of the Maximum Power Point Tracker for photovoltaic generators with Particle Swarm Optimization technique by adding repulsive force among agents. In Proceedings of the International Conference on Electrical Machines and Systems, Tokyo, Japan, 15–18 November 2009; pp. 1–6.
29. Li, F.; Deng, F.; Guo, S.; Fan, X. MPPT control of PV system under partially shaded conditions based on PSO-DE hybrid algorithm. In Proceedings of the 32nd Chinese Control Conference, Xi'an, China, 26–28 July 2013; pp. 7553–7557.
30. Vysakh, M.; Azharuddin, M.; Vilas, H.; Muralidhar, K.; Paul, D.; Jacob, B.; Babu, T.S.; Rajasekar, N. Maximum power point tracking using modified PSO with CUK Converter. In Proceedings of the International Conference on Advances in Electrical Engineering (ICAEE), Vellore, India, 9–11 January 2014; pp. 1–6.
31. Liu, J.; Li, J.; Wu, J.; Zhou, W. Global MPPT algorithm with coordinated control of PSO and INC for rooftop PV array. *J. Eng.* **2017**, *2017*, 778–782. [[CrossRef](#)]
32. Ishaque, K.; Salam, Z.; Amjad, M.; Mekhilef, S. An improved particle swarm optimization (PSO)-based MPPT for PV with reduced steady state oscillation. *IEEE Trans. Power Electron.* **2012**, *27*, 3627–3638. [[CrossRef](#)]
33. Liu, Y.H.; Huang, S.C.; Huang, J.W.; Liang, W.C. A particle swarm optimization-based maximum power point tracking algorithm for PV systems operating under partially shaded conditions. *IEEE Trans. Energy Convers.* **2012**, *27*, 1027–1035. [[CrossRef](#)]
34. Ishaque, K.; Salam, Z. A deterministic particle swarm optimization maximum power point tracker for photovoltaic system under partial shading condition. *IEEE Trans. Ind. Electron.* **2013**, *60*, 3195–3206. [[CrossRef](#)]
35. Ngan, M.S.; Tan, C.W. Multiple Peaks Tracking Algorithm using Particle Swarm Optimization Incorporated with Artificial Neural Network. *Int. J. Electron. Commun. Eng.* **2011**, *5*, 1325–1331.
36. Rajendran, S.; Srinivasan, H. Simplified accelerated particle swarm optimization algorithm for efficient maximum power point tracking in partially shaded photovoltaic systems. *IET Renew. Power Gener.* **2016**, *10*, 1340–1347. [[CrossRef](#)]
37. Alshareef, M.; Lin, Z. A Modified Particle Swarm Optimization based Maximum Power Point Tracking for PV Systems. In Proceedings of the 53th International Universities Power Engineering Conference (UPEC), Glasgow, Scotland, 4–7 September 2018; pp. 1–6.



© 2019 by the authors. Licensee MDPI, Basel, Switzerland. This article is an open access article distributed under the terms and conditions of the Creative Commons Attribution (CC BY) license (<http://creativecommons.org/licenses/by/4.0/>).